Journal of the Physical Society of Japan
Vol. 67, No. 11, November, 1998, pp. 3794-3800

Stabilization of Resistive Wall Mode Due to Shear Alfvén Resonance in a Cylindrical Plasma with a Uniform Longitudinal Flow

Akira YOSHIOKA, Tomoya TATSUNO and Masahiro WAKATANI

Department of Fundamental Energy Science, Graduate School of Energy Science, Kyoto University, Gokasho, Uji 611-0011

(Received June 29, 1998)

Resistive wall mode (RWM) is studied in a cylindrical plasma with a uniform longitudinal plasma flow. In order to simplify the analysis, two steps current profile model is employed with a constant current density j_0 for the inner region $0 \leq r \leq a_0$ and a constant current density j_1 for the outer region $a_0 \leq r \leq a$. Also the resistive shell is assumed sufficiently thin. Current profiles from peaked ones to hollow ones are simulated by changing the ratio j_1/j_0. Based on the incompressible MHD model, it is shown that RWM can be stabilized by adjusting the resistive wall position, when the shear Alfvén resonance appears inside the plasma column, with the increase of the uniform flow velocity. In this case the free energy destabilizing the RWM is absorbed in the plasma column through the shear Alfvén resonance. However, except when the RWM is close to the marginal state without a plasma flow, the flow velocity for stabilization is comparable to the sound velocity.

KEYWORDS: MHD instability, cylindrical tokamak model, resistive wall mode, shear Alfvén resonance, uniform plasma flow

§1. Introduction

The ideal MHD stability of a cylindrical diffuse plasma surrounded by a vacuum region and an ideal conducting wall was completely analyzed by Newcomb.[1] A similar cylindrical plasma model applicable to a large aspect ratio tokamak was studied by Shafranov[2] for ideal and resistive MHD modes. Resistive tearing modes were studied intensively by Furth, Rutherford and Selberg[3] for different diffuse current profiles in a cylindrical tokamak. These results were reviewed by Wesson.[4] Based on these studies it is shown that the simple cylindrical plasma model is useful to study MHD stability of circular cross-section tokamak, particularly for low beta plasmas.

Recent interest of the tokamak MHD stability is in the rotational effect on the ideal and resistive kink modes, particularly when the ideal conducting wall is replaced with the resistive wall.[5] Here the kink mode appears when the resonant surface r_s satisfying $q(r_s) = m/n$ exists at the outside of plasma column, where $m(n)$ is a poloidal (toroidal) mode number and q is a safety factor. There are some experimental results showing importance of plasma rotation in tokamak plasmas. One is the H(high)-mode[6] with the edge transport barrier and the other is the high-β_p mode[7] or negative (reversed) shear mode[8] with the internal transport barrier. There exists positive correlation between the improvement of confinement and the generation of plasma rotation.[9] After the L-H transition, density fluctuations were suppressed substantially; however, sometimes the edge localized modes (ELMs) were excited.[10] Another example is the observation of locked mode.[11] When the toroidal plasma rotation was suppressed, MHD fluctuations were enhanced, which led to the major disruption occasionally. It is a practical way to stabilize the major disruption due to the locked mode with the plasma rotation induced by the neutral beam injection.[12]

It was pointed out that there is an interaction between the resistive wall and the plasma rotation for the MHD stability.[13,14] The stability of the resistive wall mode (RWM) depends on the position of resistive wall in the cylindrical model. It was shown that the RWM appears when the resistive wall was sufficiently close to the plasma column. By comparing tokamak stability results with the RWM theory, it seems that the RWMs are more stable than predicted theoretically for the cylindrical tokamak. For the toroidal plasma model, it was shown that the coupling of toroidicity and plasma rotation may suppress the RWMs.[15] For the cylindrical model, it was also shown that the magnetosonic resonance appeared in the linearized MHD eigenvalue equation had a significant stabilizing effect on RWMs in the presence of longitudinal plasma flow.[16] In this paper we will point out that the shear Alfvén resonance in the linearized MHD eigenvalue equation has a stabilizing effect on RWMs, which occurs for $\omega - \Omega = \omega_A$, where ω is a mode frequency, $\Omega = -(n/R)V_0$ and $\omega_A^2 = (B_\theta/r)^2(m-nq)^2/(\mu\rho_0)$. Here V_0 is a uniform longitudinal flow velocity, $2\pi R$ is a periodic length in the z direction, ρ_0 is a uniform plasma density, and B_θ an azimuthal magnetic field due to a longitudinal current $j_z(r)$.

We use a simple cylindrical plasma model given by Glasser, Furth and Rutherford[17] to demonstrate the stabilization of RWMs by the shear Alfvén resonance in the presence of uniform flow as shown in Fig. 1. The current profile is composed of two uniform current density regions as shown in Fig. 2. There are two surfaces with the jump of current density at $r = a_0$ and $r = a$. The re-

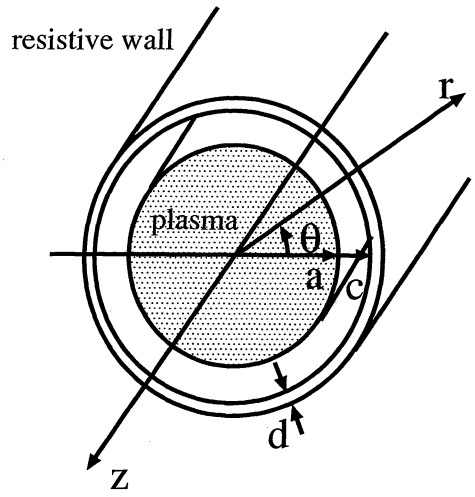

Fig. 1. A cylindrical plasma model surrounded by a vacuum region in $a < r < c$ and a thin resistive wall of a width d. Here (r, θ, z) is a cylindrical coordinates.

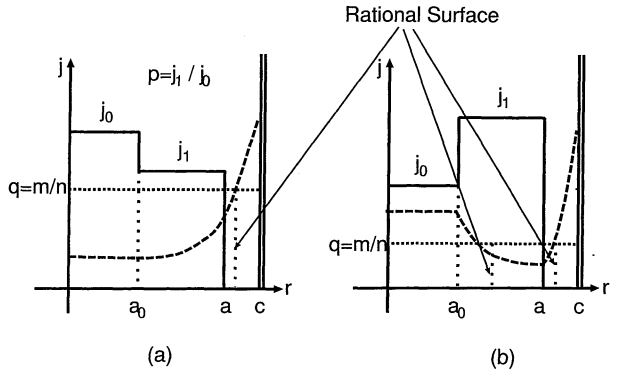

Fig. 2. A model of longitudinal plasma current profile $j_z(r)$. The broken line denotes the safety factor profile. (a) Corresponds to positive shear case, and (b) Corresponds to negative shear case. The current jump occurs at $r = a_0$ and $r = a$. The thin resistive wall is located at $r = c$.

sistive wall is located at $r = c$. The current ratio is given by $p = j_1/j_0$. In Fig. 2, safety factor profiles are shown for the cases with $p < 1$ and $p > 1$. The former case corresponds to the positive shear[7] and the latter case to the negative shear.[8] This negative shear configuration is a special case, since $q_{\min} = q_a$, where $q_{\min}$ denotes the minimum of safety factor and q_a denotes the surface q value. In §2 we show the linearized MHD eigenvalue equation for the cylindrical plasma with a uniform longitudinal flow associated with boundary conditions. In §3 we show both the growth rate and mode frequency for the RWM with $(m, n) = (2, 1)$ as a function of the resistive wall position. When c is close to a, the existence of RWM is clearly seen.[5] The stability of RWM is checked for various current profiles by changing the parameter p. Next we increase the longitudinal flow velocity. In this case we obtain the stabilizing tendency of RWM. In §4 we analyze the reason why the growth rate vanishes for a longitudinal flow velocity exceeding a threshold value. In §5 it is confirmed that the shear Alfvén resonance is an important ingredient for stabilizing RWM, which is similar to the shear Alfvén wave heating by applying an oscillating helical coil current.[18,19] Finally concluding remarks will be given in §6.

§2. Linear MHD Stability of a Cylindrical Plasma with a Uniform Longitudinal Flow

For a cylindrical tokamak plasma model with an equilibrium magnetic field $\mathbf{B} = (0, B_\theta(r), B_0)$, the linearized ideal MHD equation can be written as[20]

$$\frac{\mathrm{d}}{\mathrm{d}r}\left[\frac{r}{\omega_A^2}(\omega_A^2 - \bar{\omega}^2)\frac{\mathrm{d}\psi}{\mathrm{d}r}\right] - \frac{1}{\sqrt{\mu_0\rho}}\frac{m}{\omega_A}\frac{\mathrm{d}}{\mathrm{d}r}\left[(1-A^2)j_z + 2A^2\frac{B_\theta}{r}\right]\psi - \frac{m^2}{r}(1-A^2)\psi = 0\,, \tag{2.1}$$

in the cylindrical coordinates (r, θ, z), where $\bar{\omega} = \omega - \Omega$, $\Omega = -(n/R)V_0$, $\omega_A^2 = F^2/\mu_0\rho$, $F = (B_\theta/r)(m - nq)$, and $A^2 = \bar{\omega}^2/\omega_A^2$. Here V_0 is a uniform flow velocity in the z direction, j_z is a plasma current in the z direction and $q = (r/R)(B_0/B_\theta)$ is a safety factor. The perturbed magnetic field is given by $\tilde{\mathbf{B}} = \nabla\tilde{\psi} \times \hat{z}$ and $\tilde{\psi}(r, \theta, z, t) = \psi(r)\exp(-\mathrm{i}\omega t + \mathrm{i}m\theta - \mathrm{i}nz/R)$ is assumed to obtain eq. (1). Also the external longitudinal magnetic field B_0 is assumed constant. It should be noted that the surface satisfying $F = 0$ or $q = m/n$ is called a resonant surface. In deriving eq. (2), the pressure effect is neglected under the low beta approximation, and the mass density ρ is assumed constant.

The stability of current-driven MHD modes is studied by solving eq. (1) as an eigen-value problem under appropriate boundary conditions. One characteristic boundary condition is related to the thin resistive wall at $r = c$, which is shown as

$$\left[\frac{r}{\psi}\frac{\mathrm{d}\psi}{\mathrm{d}r}\right]_{r=c} = \mathrm{i}\omega\tau_w, \tag{2.2}$$

where $\tau_w = cd/\eta_w$ is a skin time of the resistive wall with a thickness d. Here $[\,\cdot\,]$ in eq. (2) denotes the jump condition for the case of $d/c \ll 1$. The wall resistivity is denoted as η_w. Next we consider the boundary condition at the plasma surface $r = a$. We integrate eq. (1) in the thin layer including $r = a$, $[a - \epsilon,\ a + \epsilon]$, and take the limit of $\epsilon \to 0$ to obtain

$$\left(\frac{r}{\psi}\frac{\mathrm{d}\psi}{\mathrm{d}r}\right)_{r=a^+} = \left\{\frac{\omega_A^2 - \bar{\omega}^2}{\omega_A^2}\left(\frac{r}{\psi}\frac{\mathrm{d}\psi}{\mathrm{d}r}\right)\right\}_{r=a^-} - \frac{m}{F}\left\{(1-A^2)j_z + 2A^2\frac{B_\theta}{r}\right\}_{r=a^-}, \tag{2.3}$$

where $a^+(a^-)$ denotes $a + \epsilon(a - \epsilon)$ in the limit of $\epsilon \to 0$. Since the solution of the perturbed flux function ψ in the vacuum region is shown as $\psi = \psi_1 r^m + \psi_2 r^{-m}$ under the condition of $(m/n)^2 \gg (r/R)^2$, the boundary condition (2) gives

$$\left(\frac{r}{\psi}\frac{\mathrm{d}\psi}{\mathrm{d}r}\right)_{r=a^+} = -m\frac{1 + h(a/c)^{2m}}{1 - h(a/c)^{2m}}\,, \tag{2.4}$$

where

$$h = \left(1 + \frac{2\mathrm{i}m}{\omega\tau_w}\right)^{-1}. \tag{2.5}$$

Here ψ_1 and ψ_2 are constants. Finally the boundary condition at the axis of cylindrical plasma column is

$$\psi(r) \propto r^m, \tag{2.6}$$

for the (m,n) mode.

§3. Numerical Scheme for Obtaining Eigenvalue and Eigenfunction

We solved eq. (1) as the eigenvalue problem with the boundary conditions (3), (4) and (6) by employing a shooting method. Since the eigenvalue is complex, we also use Newton method in the two-dimensional space. For obtaining solutions (ω,γ) satisfying $f(\omega,\gamma) = 0$ and $g(\omega,\gamma) = 0$, we use the following relations between guessed values (ω_g,γ_g) and corrected values $(\omega = \omega_g + \Delta\omega,\ \gamma = \gamma_g + \Delta\gamma)$,

$$f(\omega_g,\gamma_g) - \left.\frac{\partial f}{\partial\omega}\right|_{\omega=\omega_g}\Delta\omega - \left.\frac{\partial f}{\partial\gamma}\right|_{\gamma=\gamma_g}\Delta\gamma = 0 \tag{3.1}$$

$$g(\omega_g,\gamma_g) - \left.\frac{\partial g}{\partial\omega}\right|_{\omega=\omega_g}\Delta\omega - \left.\frac{\partial g}{\partial\gamma}\right|_{\gamma=\gamma_g}\Delta\gamma = 0. \tag{3.2}$$

Explicit expressions of f and g are given by

$$f = \mathrm{Re}\left[\left(\frac{r}{\psi}\frac{\mathrm{d}\psi}{\mathrm{d}r}\right)_{r=a+} - \left\{\frac{\omega_A^2-\bar{\omega}^2}{\omega_A^2}\left(\frac{r}{\psi}\frac{\mathrm{d}\psi}{\mathrm{d}r}\right)\right\}_{r=a-} - \frac{m}{F}\left\{(1-A^2)j_z + 2A^2\frac{B_\theta}{r}\right\}_{r=a-}\right], \tag{3.3}$$

$$g = \mathrm{Im}\left[\left(\frac{r}{\psi}\frac{\mathrm{d}\psi}{\mathrm{d}r}\right)_{r=a+} - \left\{\frac{\omega_A^2-\bar{\omega}^2}{\omega_A^2}\left(\frac{r}{\psi}\frac{\mathrm{d}\psi}{\mathrm{d}r}\right)\right\}_{r=a-} - \frac{m}{F}\left\{(1-A^2)j_z + 2A^2\frac{B_\theta}{r}\right\}_{r=a-}\right]. \tag{3.4}$$

Here $\{(r/\psi)(\mathrm{d}\psi/\mathrm{d}r)\}_{r=a-}$ can be obtained by solving eq. (1) numerically with a Runge-Kutta method for the assumed values (ω_g,γ_g).

In order to check the above numerical scheme to obtain the eigenvalue, our results are compared with the analytic expression given by Finn[5]

$$\bar{\omega}^2 = -\frac{\gamma_\infty^2 + R(\omega)\gamma_c^2}{1+R(\omega)} \tag{3.5}$$

for the uniform current density case in Fig. 2 or the $p = 1$ case, where

$$R(\omega) = -\frac{1}{2}\left(1 - \frac{a^{2m}}{c^{2m}}\right)\frac{\mathrm{i}\omega\tau_w}{m}, \tag{3.6}$$

$$\gamma_c^2(c) = \frac{2B_0^2}{\rho R^2 q_a^2}\frac{m-nq_a}{1-a^{2m}/c^{2m}} \times (1 - a^{2m}/c^{2m} - m + nq_a) \tag{3.7}$$

and $\gamma_\infty^2 = \gamma_c^2(c\to\infty)$. The safety factor at $r = a$ is denoted by q_a. For the case with $p = 1$, $a_0/a = 1$, $q_a = 1.5$ and $\Omega = 0.5$, numerical growth rates show good agreement with eq. (11) with relative errors less than 10^{-5} as shown in Fig. 3. Here other parameters $(m,n) = (2,1)$, $R/a = 5$, $d/a = 0.02$, and $\eta_w/a = 10^{-4}(\Omega)$. The RWM is seen for $c/a \lesssim 1.18$, since the instability for $c/a > 1.18$ is essentially same as the ideal kink mode.

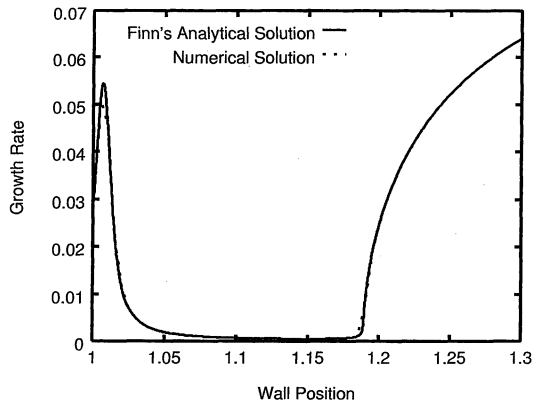

Fig. 3. Growth rates as a function of c/a for $p = 1$, $a_0/a = 1$, $q_a = 1.5$, $\Omega = 0.5$, $R/a = 5$, $d/a = 0.02$ and $\eta_w/a = 10^{-4}(\Omega)$. Mode numbers are $(m,n) = (2,1)$.

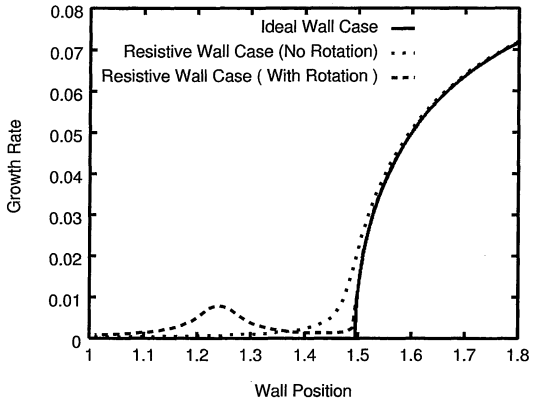

Fig. 4. Growth rates of ideal kink mode and resistive wall mode (RWM) are shown as a function of c/a. Mode numbers are $(m,n) = (2,1)$ and $q_a = 1.2$, $\Omega = 0.13$, $p = 1$. Growth rates of RWM are also shown for $\Omega = 0$ case.

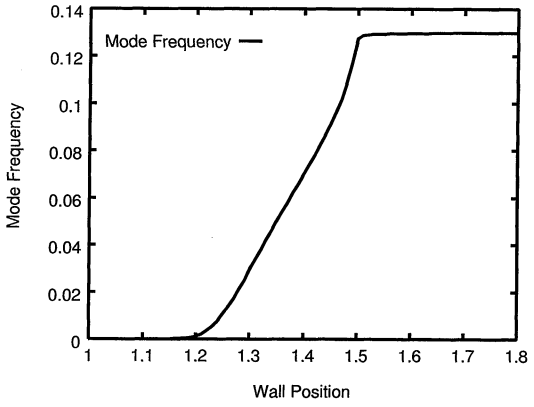

Fig. 5. Angular frequency of resistive wall mode (RWM) in case of longitudinal uniform flow ($\Omega = 0.13$) as a function of c/a. Other parameters are the same as those in Fig. 4.

For the case of $q_a = 1.2$, $p = 1.0$ and $\Omega = 0.13$, growth rates and mode frequencies are shown in Figs. 4 and 5, respectively. In Fig. 4 the $(m,n) = (2,1)$ mode is suppressed when $c/a \le 1.5$ for the ideal wall case; however, for the resistive wall case without the uniform longitudinal flow or plasma rotation, the $(m,n) = (2,1)$ mode becomes unstable with residual growth rates even for

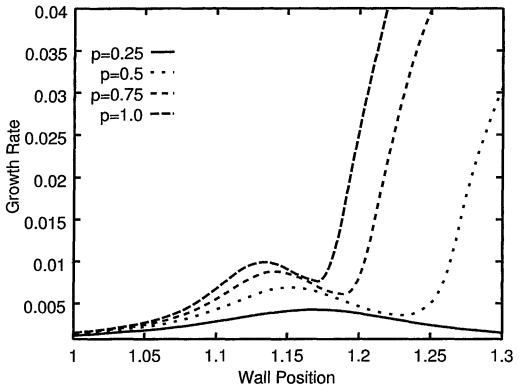

Fig. 6. Current profile effect on growth rates of RWM with $(m,n) = (2,1)$ as a function of c/a for $q_a = 1.5$, $a_0/a = 0.5$, $\Omega = 0.07$. Current profile is changed with the parameter p.

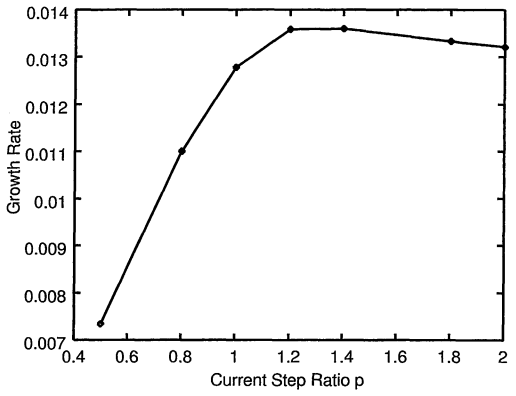

Fig. 7. Growth rates of RWM as a function of p for $q_a = 1.8$, $a_0/a = 0.5$, $\Omega = 0.01$ and $c/a = 1.04$. For $p > 1$, the current profile becomes hollow and negative shear appears.

$c/a \leq 1.5$. When the plasma rotation is included in the resistive wall case, the growth rates for $1.36 \lesssim c/a \lesssim 1.5$ are decreased. However, for $c/a \lesssim 1.36$, the growth rates are enhanced. These are characteristics of RWM in the presence of the uniform longitudinal flow. Figure 5 shows that the mode frequency of RWM increases almost linearly for $c/a \gtrsim 1.2$. When the ideal kink mode becomes unstable for $c/a > 1.5$, the mode frequency becomes constant and equal to $\Omega = 0.13$ which is determined by the longitudinal flow velocity V_0.

Figure 6 shows the current profile effect on the growth rate of RWM, where p is changed from 0.25 to 1.0 for $q_a = 1.5$, $a_0/a = 0.5$ and $\Omega = 0.07$. The peaked current profile case with $p = 0.25$ gives the smallest growth rate as a function of c/a. When the current profile becomes flat with the increase of p, the RWM becomes unstable and the ideal kink branch appears. The current profile model shown in Fig. 2 may describe negative shear configurations for $p > 1$. Figure 7 shows growth rates of RWM for $p > 0.5$ with c/a fixed at 1.04. The growth rate saturates and decreases gradually for $p \gtrsim 1.0$. It seems that the negative shear configuration has no significant stabilizing effect on the resistive wall mode in the presence of longitudinal flow. We also confirmed this result for smooth hollow current profiles.

§4. Stabilization of Resistive Wall Mode with Shear Alfvén Resonance

In this section we concentrate in the longitudinal flow velocity effect on the growth rates of resistive wall mode. As shown in Fig. 8, growth rates of RWM decrease and become negative for $1.043 < c/a < 1.055$ for $\Omega = 0.075$. In Fig. 9, eigenfunctions corresponding to wall positions shown in Fig. 8 are shown for several cases of c/a. The most peaked eigenfunction is obtained for $c/a = 1.043$. Also for $c/a = 1.055$ the eigenfunction is peaked. These profiles suggest existence of resonant behavior at $r/a = 0.8076$ for $c/a = 1.043$ and at $r/a \simeq 0.9808$ for $c/a = 1.055$. The eigenvalues are $\omega_A^2 - \bar{\omega}^2 = (-4.33 \times 10^{-4},\ 1.89 \times 10^{-3})$ for $c/a = 1.043$ and $\omega_A^2 - \bar{\omega}^2 = (-2.5 \times 10^{-2},\ 7.37 \times 10^{-2})$ for $c/a = 1.055$. These eigenvalues suggest $\omega_A^2 - \bar{\omega}^2 = 0$ for the resonant condition. This corresponds to appearance of the regular singular point in the second-order differential equation (1), which is called shear Alfvén resonance in the MHD theory. It should be noted that Ω plays an important role to satisfy $\omega_A^2 - \bar{\omega}^2 = 0$, since $\bar{\omega}^2 = (\omega - \Omega)^2$. When $\omega_A^2 - \bar{\omega}^2 = 0$ is satisfied at $r = r_0$, the Frobenius solution in the neighborhood of $r = r_0$ is written as

$$\psi(r) = [\psi_1 + \psi_2 \ln(r_0 - r)][1 - c_1(r_0 - r)] + 2\psi_2 c_1 (r_0 - r), \tag{4.1}$$

where

$$c_1 = \left[\frac{\omega_A^2}{(\omega_A^2)' r}\right]\Bigg|_{r=r_0} \times \left[\frac{m}{F}\frac{\mathrm{d}}{\mathrm{d}r}\left\{(1 - A^2) j_z + 2A^2 \frac{B_\theta}{r}\right\}\right]\Bigg|_{r=r_0}. \tag{4.2}$$

In eq. (14), ψ_1 and ψ_2 are constants determined by connection conditions to the external solutions far from $r = r_0$. The Frobenius solution suggests existence of logarithmic singularity in the eigenfunction.

In the numerical calculations the Frobenius solution is connected with the external solutions in the regions $[0,\ r_0 - \epsilon]$ and $[r_0 + \epsilon,\ a]$ at $r = r_0 \pm \epsilon$. In particular, for the marginally stable case, the eigenfunction ψ_- is real in $[0,\ r_0 - \epsilon]$. At $r = r_0 - \epsilon$ the connection conditions that ψ and ψ' are continuous give

$$\psi_-(r_0 - \epsilon) = (\psi_1 + \psi_2 \ln\epsilon)(1 - c_1\epsilon) + 2\psi_2 c_1 \epsilon, \tag{4.3}$$

$$\psi'_-(r_0 - \epsilon) = +c_1(\psi_1 + \psi_2 \ln\epsilon) - (\psi_2/\epsilon)(1 - c_1\epsilon) - 2\psi_2 c_1, \tag{4.4}$$

where the prime denotes the radial derivative. When ϵ is given, ψ_1 and ψ_2 can be determined from eqs. (16) and (17). For the connection conditions at $r = r_0 + \epsilon$, we need the relation obtained by the analytic continuation

$$\ln(-\epsilon) = \ln(\epsilon) \pm \mathrm{i}\pi. \tag{4.5}$$

The sign of the second term in the RHS of eq. (18) depends on the current profile. Since $\Omega - \omega = \omega_A(r_s)$ is satisfied at the singular point,

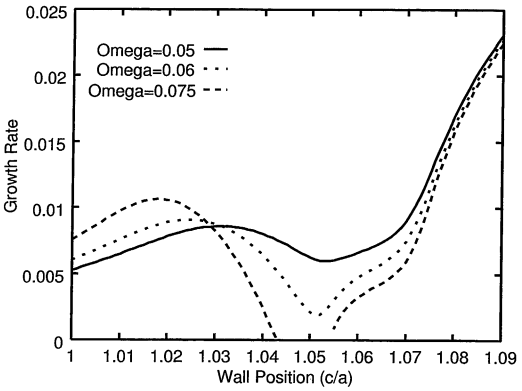

Fig. 8. Dependence of growth rates of RWM with $(m,n) = (2,1)$ on the resistive wall position c/a for the several angular frequencies $\Omega = -V_0/R = 0.05$, 0.06 and 0.075, where V_0 is a longitudinal flow velocity. Other parameters are $q_a = 1.8$, $a_0/a = 0.5$ and $p = 0.5$.

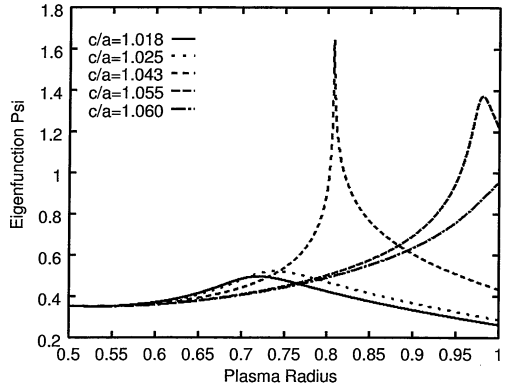

Fig. 9. Radial profiles of eigenfunction $\psi(r)$ for the $(m,n) = (2,1)$ mode in cases of $c/a = 1.018$, 1.025, 1.043, 1.055 and 1.066. Other parameters are $q_a = 1.8$, $a_0/a = 0.5$, $p = 0.5$ and $\Omega = 0.075$.

$$\Omega - \mathrm{Re}(\omega) = \frac{\mu_0\, m\, a_0^2 (j_0 - j_1)(\alpha^2 - \beta^2)}{2(\alpha^2-\beta^2)^2 + 8\alpha^2\beta^2} + \frac{\mu_0 m j_1}{2} - \frac{nB_0}{R} \tag{4.6}$$

$$\mathrm{Im}(\omega) = \frac{\mu_0\, m\, a_0^2 (j_0 - j_1)\alpha\beta}{(\alpha^2-\beta^2)^2 + 4\alpha^2\beta^2}. \tag{4.7}$$

for a complex variable $r_s = \alpha + \mathrm{i}\beta$ with $\alpha > 0$. When the current profile is peaked or $j_0 > j_1$, eq. (20) gives $\beta > 0$ ($\beta < 0$) for $\mathrm{Im}(\omega) > 0$ ($\mathrm{Im}(\omega) < 0$). Thus $-\mathrm{i}\pi$ is appropriate in the analytic continuation in eq. (18) for $j_0 > j_1$. On the contrary, we take $+\mathrm{i}\pi$ for $j_0 < j_1$ or hollow current cases.

Since the external solution in $[r_0 + \epsilon,\ a]$ becomes complex, $\psi_+ = \psi_{+R} + \mathrm{i}\psi_{+I}$, the connection conditions at $r = r_0 + \epsilon$ give

$$\psi_{+R}(r_0+\epsilon) + \mathrm{i}\psi_{+I}(r_0+\epsilon) = (\psi_1 + \psi_2 \ln\epsilon - \mathrm{i}\pi\psi_2)(1 + c_1\epsilon) - 2\psi_2 c_1 \epsilon \tag{4.8}$$

$$\psi'_{+R}(r_0+\epsilon) + \mathrm{i}\psi'_{+I}(r_0+\epsilon) = c_1(\psi_1 + \psi_2 \ln\epsilon - \mathrm{i}\pi\psi_2) + \frac{\psi_2}{\epsilon}(1 + c_1\epsilon) - 2\psi_2 c_1. \tag{4.9}$$

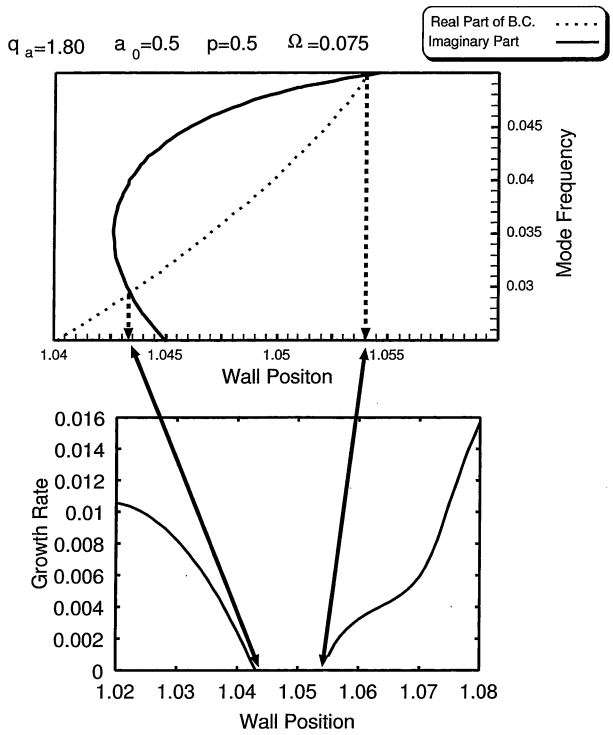

Fig. 10. The upper figure shows $f(\omega,0) = 0$ (dotted line) and $g(\omega,0) = 0$ (continuous line) in $(\omega, c/a)$ plane, where ω is the real mode frequency and c/a is the normalized position of resistive wall. The lower figure shows growth rates of RWM with $(m,n) = (2,1)$ as a function of c/a. Other parameters are $q_a = 1.8$, $a_0/a = 0.5$, $p = 0.5$ and $\Omega = 0.075$.

Here ψ_{+R}, ψ_{+I}, ψ'_{+R} and ψ'_{+I} can be calculated, since ψ_1 and ψ_2 are already determined. For the solution in $[r_0 + \epsilon,\ a]$, these given values become initial conditions of the Runge-Kutta solver. From this numerical solution, the logarithmic derivative at the surface of plasma column $(r\psi'/\psi)|_{r=a-}$ is obtained. For the marginally stable case, the position of resistive wall and the mode frequency are given to satisfy the boundary condition at $r = a$ (3). The upper figure in Fig. 10 shows two lines describing $f(\omega,0) = 0$ and $g(\omega,0) = 0$ in the $(\omega, c/a)$ plane. When these two curves are crossed in this plane, the point corresponds to the marginal stability of RWM. There are two cross points, and each point corresponds to the marginal stability case in Fig. 8 as shown by the lower figure in Fig. 10. These results mean that the RWM with $(m,n) = (2,1)$ is stabilized for $1.043 < c/a < 1.055$ due to the shear Alfvén resonance which absorbs the free energy for exciting RWM. It is noted that the density profile affects the resonance condition, since the Alfvén velocity depends on density. Thus the density profile is important for evaluating the stability condition quantitatively.

§5. Properties of Shear Alfvén Resonance

Since the Alfvén resonance appears only for a rotating plasma with $\Omega \neq 0$, it is important to estimate the minimum rotational frequency Ω or the minimum flow velocity V_0 for suppressing the RWM. With the two steps current profile model shown in Fig. 2, the marginal values of Ω for appearance of shear Alfvén resonance in the case of

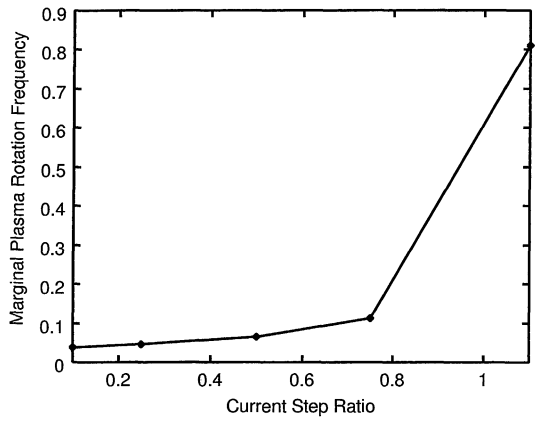

Fig. 11. Dependence of marginal rotational frequency Ω on p to suppress RWM with $(m,n) = (2,1)$ due to shear Alfvén resonance for $q_a = 1.8$ and $a_0/a = 0.5$.

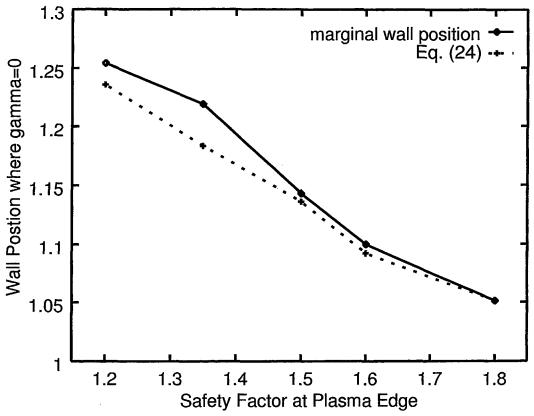

Fig. 12. Resistive wall position for the marginal rotational frequency case is shown as a function of q_a with black circles. The dotted line corresponds to eq. (24). Here RWM has the mode numbers $(m,n) = (2,1)$, $p = 0.5$ and $a_0/a = 0.5$.

$(m,n) = (2,1)$ are plotted in Fig. 11 as a function of p for $q_a = 1.8$ and $a_0/a = 0.5$. Here the marginal rotational frequency case corresponds to that just one particular resistive wall position makes the RWM marginal. The RWM is still unstable for other resistive wall positions. Figure 11 shows that the minimum value of $\Omega = 0.03$ is obtained for $p = 0.1$, $q_a = 1.8$ and $a_0/a = 0.5$, which corresponds to the case that the ideal kink mode with $(m,n) = (2,1)$ is almost marginal even without the ideal conducting wall. It is noted that $\Omega = 0.03$ gives $V_0 = 3.4 \times 10^5$(m/s) for $a = 1$m, $R = 5$m, $B_0 = 1$T and $n_e = 10^{20}(\mathrm{m}^{-3})$. Even for a high density plasma, the longitudinal flow velocity V_0 is a few times larger than the typical toroidal flow velocity in the present large tokamaks such as JT-60U and JET. As a reference an ion sound velocity C_s is given for a deuterium plasma, $C_s = 3.5 \times 10^5$(m/s) at $T_e = 2.5$keV. Thus V_0 seems comparable to C_s.

From the above numerical results, the RWM may be stabilized when the Alfvén resonance appears inside the plasma column with the increase of the rotational frequency Ω. From Figs. 8 and 9, it is expected that the right hand side of the stability window with the widest region corresponds to the situation that the shear Alfvén resonance is located at $r = a$. When the Alfvén resonance exists at the plasma surface, $(\omega - \Omega)^2 = (\omega_A(a))^2$ is satisfied. Substituting this relation into eq. (3) yields

$$\left(\frac{r}{\psi}\frac{\mathrm{d}\psi}{\mathrm{d}r}\right)_{r=a+} = -\frac{2m}{m - nq_a} . \tag{5.1}$$

Since $\omega\tau_w \gg 1$ for eq. (5), $h \simeq 1$ is obtained in eq. (4). Then from eqs. (4) and (23), we obtain

$$\frac{c}{a} = \left(\frac{2 + m - nq_a}{2 - m + nq_a}\right)^{1/2m} . \tag{5.2}$$

Figure 12 shows the resistive wall position for the marginal rotational frequency case as a function of q_a. For comparison eq. (24) is plotted with the dotted line. The resistive wall position given by eq. (24) should be larger than the black circles in Fig. 12, since eq. (24) corresponds to the widest stability window case. However, the approximate relation (24) gives a little lower c/a, which comes from the assumptions in the derivation of eq. (24). In spite of this fact, it may be considered that eq. (24) predicts existence of marginal stability of RWM due to the longitudinal uniform flow fairly well.

§6. Concluding Remarks

Recent topic for the improved confinement in tokamaks is the study of negative (reverse) shear configuration. When the confinement was improved by generating the internal transport barrier, large toroidal rotation velocity was usually observed in the negative or weak shear region. Although the physical mechanism for generating the transport barrier is not fully clarified, the MHD stability of the negative shear configuration with the plasma rotation is an interesting subject. In the negative shear region the ideal ballooning modes or interchange modes become stable, while the resistive interchange modes become unstable.[21,22]

It is pointed out that the resistive wall modes (RWMs) or the kink modes unstable in the presence of the resistive wall can be destabilized by the toroidal plasma flow. However, in tokamak experiments, RWMs were not clearly observed, which suggested existence of stabilizing mechanisms neglected in the MHD model particularly for the cylindrical tokamak plasma. Theories have been developed for the coupling between the RWM and sound wave due to compressibility[16] and the coupling between the RWM and stable MHD mode due to toroidicity.[15] In addition to these possibilities, the shear Alfvén resonance has been shown to stabilize the RWM even in the cylindrical tokamak plasma model. The resonance condition is $(\omega - \Omega)^2 = \omega_A^2$, where $\Omega = -(n/R)V_0$ is the rotational frequency due to the uniform longitudinal flow velocity V_0 and $\omega_A^2 = \{(B_\theta/r)(m - nq)\}^2/\mu_0\rho$. Here $m(n)$ is the poloidal (toroidal) mode number, q is the safety factor, B_θ is the poloidal magnetic field, and ρ is a uniform plasma density. When the surface satisfying $(\omega - \Omega)^2 = \omega_A^2$ appears in the plasma column with the increase of V_0, the shear Alfvén resonance becomes effective to stabilize the RWM. This stabilizing mechanism has been confirmed numerically in this paper. However, in order to realize the stabilization of RWM, the resis-

tive wall position is restricted, which is fairly close to the plasma column. The magnitude of the longitudinal flow velocity to generate the shear Alfvén resonance depends on the conducting wall position to stabilize the ideal kink mode. When the ideal kink mode has a stabilizing tendency due to a peaked current profile, the toroidal flow velocity for stabilizing RWM is decreased.

According to our simple two steps current profile model, it is shown that the negative shear configuration or the hollow current profile case is vulnerable to the RWM. It seems necessary to study the stability of RWM in the negative shear configuration carefully for optimizing the safety factor profile. Also it will be necessary to include the finite beta effect in the toroidal geometry for the stability analysis considering the shear Alfvén resonance to estimate rotational frequency at the marginal state, which will be a future study.

1) W. A. Newcomb: Ann. Phys. **3** (1958) 347.
2) V. D. Shafranov: Sov. Phys. Tech. Phys. **15** (1970) 175.
3) H. P. Furth *et al.*: Phys. Fluids **16** (1973) 1054.
4) J. A. Wesson: Nucl. Fusion **18** (1978) 87.
5) J. M. Finn: Phys. Plasmas **2** (1995) 198.
6) F. Wagner *et al.*: Phys. Rev. Lett. **49** (1982) 1408.
7) Y. Koide *et al.*: Phys. Rev. Lett. **72** (1994) 3662.
8) T. Fujita *et al.*: Phys. Rev. Lett. **78** (1997) 2377.
9) K. Ida *et al.*: Phys. Rev. Lett. **65** (1990) 1364.
10) K. H. Burrel *et al.*: Plasma Phys. Control. Fusion **31** (1989) 1649.
11) H. Ninomiya *et al.*: Nucl. Fusion **28** (1988) 1275.
12) R. J. La Haye *et al.*: Phys. Fluids B **4** (1992) 2098.
13) Z. Yoshida and N. Inoue: Plasma Phys. Control. Fusion **27** (1985) 245.
14) T. C. Hender *et al.*: Nucl. Fusion **29** (1989) 1279.
15) A. Bondeson and D. J. Ward: Phys. Rev. Lett. **72** (1994) 2709.
16) R. Betti and J. P. Freidberg: Phys. Rev. Lett. **74** (1995) 2949.
17) A. H. Glasser *et al.*: Phys. Rev. Lett. **38** (1997) 234.
18) J. A. Tataronis and W. Grossmann: Z. Phys. **261** (1973) 203.
19) L. Chen and A. Hasegawa: Phys. Fluids **17** (1974) 1399.
20) C. G. Gimblett *et al.*: Phys. Plasmas **3** (1996) 3619.
21) M. S. Chu *et al.*: Phys. Rev. Lett. **77** (1996) 2710.
22) M. Furukawa: Master thesis, Department of Nuclear Engineering, Kyoto University, Kyoto, 1998.